Journal of Materials Chemistry C

ROYAL SOCIETY OF CHEMISTRY

PAPER

View Article Online
View Journal

Cite this: DOI: 10.1039/d5tc04036a

Theoretical screening of Co- and Mo-based binary alloys as interconnect metals

Seongwoo Kang, Shinyeong Park and Jiwon Chang *

With continued device scaling, the use of copper (Cu) as an interconnect material has reached its limit for two main reasons. First, electron–phonon scattering, which dominates in the bulk form, becomes overshadowed by surface roughness and grain boundary scattering as the dimensions shrink. Second, electromigration becomes increasingly severe under high electric fields, compromising reliability. Each of these degradation factors can be quantitatively evaluated using the figure of merit (FoM) and cohesive energy. In the search for next-generation interconnect materials, Co- and Mo-based binary alloys were investigated using density functional theory (DFT) calculations combined with Boltzmann transport theory. The directionally averaged FoM and cohesive energy were computed as indicators of size-dependent resistivity and electromigration resistance, respectively. By applying screening criteria—cohesive energy greater than 5.5 eV per atom and FoM less than 6.70×10^{-16} Ω m^2 (the FoM of Cu)—four promising Co-based alloys and seven Mo-based alloys were identified. These results highlight the strong potential of Co- and Mo-based binary alloys for future interconnect applications. Furthermore, similarities in Fermi surfaces, coupled with the FoM analysis, validate these alloys as suitable candidates for advanced interconnect technologies.

Received 13th November 2025,
Accepted 30th January 2026

DOI: 10.1039/d5tc04036a

rsc.li/materials-c

Introduction

With the continued downscaling of interconnect metals into the sub-10 nm regime, metal resistivity becomes increasingly dominated by surface roughness (SR) and grain boundary (GB) scattering, rather than phonon scattering, due to pronounced size effects, as described in eqn (1). Based on the Boltzmann transport equation, Fuchs and Sondheimer[1,2] and Mayadas and Shatzkes[3,4] developed classical models for SR and GB scatterings, respectively. These models were combined,[5] as in eqn (1)

$$\rho = \rho_0 + \rho_0\lambda\frac{3(1-p)}{4d} + \rho_0\lambda\frac{3R}{2D(1-R)} \quad (1)$$

where ρ_0 is the bulk resistivity, λ is the electron mean free path, p is the surface specularity parameter, d is the line width, R is the grain boundary reflection coefficient, and D is the grain size. As presented in eqn (1), for scaled interconnect metals with reduced d and D, $\rho_0\lambda$ (figure-of-merit, FoM) serves as a key scaling parameter. Thus, numerous efforts have been focused on the search for new interconnect metals with small $\rho_0\lambda$, which is defined as:

$$\frac{1}{\rho_0\lambda} = \frac{e^2}{4\pi^3\hbar}\sum_n \iint_{S_F}\frac{v_{n,t}{}^2(\boldsymbol{k})}{|v_n(\boldsymbol{k})|^2}\mathrm{d}S \quad (2)$$

under the constant λ approximation, where $v_{n,t}$ is the electron velocity along the transport direction t. Using first-principles methods, numerous approaches have been made to predict $\rho_0\lambda$ for various materials.[6–10] High-throughput density functional theory (DFT) calculations have identified candidates for thin films and wires,[7] MAX-phase ceramics,[8] and van der Waals 2D metallic materials.[9] Moreover, machine-learning techniques have also been adopted.[10]

Cohesive energy, the energy needed to separate bulk atoms into isolated ones, reflects atomic bonding strength and is also widely used as a screening parameter. Interconnect metals with higher cohesive energy are more resistant to electromigration induced failure.[11,12]

Recently, the search for alternative metals has intensified to address the scaling limitations of copper (Cu).[13] In particular, cobalt (Co) and molybdenum (Mo) are promising due to their lower FoM and higher cohesive energies compared to Cu.[6,11] Moreover, both metals are compatible with conventional back-end-of-line processes.[13–16] Other materials that exhibit sufficiently high cohesive energy and superior FoM suffer from inherent drawbacks. Ir and Rh are prohibitively expensive, Ag is prone to agglomeration at elevated temperatures, W requires a complex barrier/liner structure, Os suffers from volatility and toxicity concerns, Ni exhibits poor thermal stability,[17] and Ru still faces challenges within large scale-manufacturing with relatively complex processes.[18–21] In this work, rather than focusing on single elemental metals, we investigate binary alloys based on Co and Mo, which are already adopted in current semiconductor fabrication processes. We theoretically assess Co- and Mo-based binary alloys, targeting candidates

Department of System Semiconductor Engineering, Yonsei University, Seoul 03722, South Korea. E-mail: jiwonchang@yonsei.ac.kr

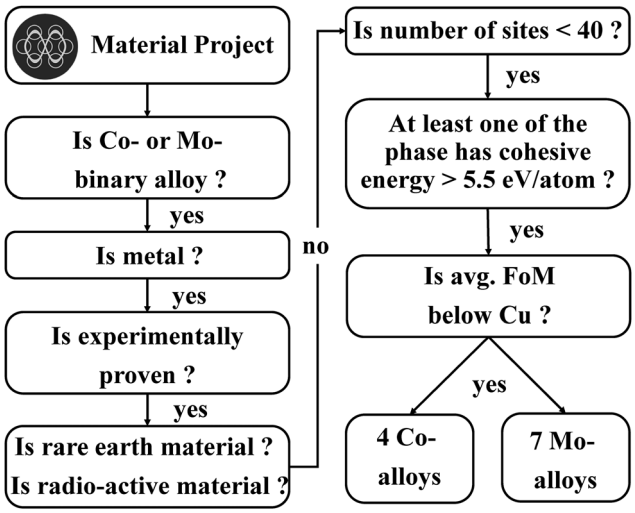

Fig. 1 Flow chart of screening promising Co-, Mo-binary alloys.

that exhibit FoM and cohesive energy values better than Cu as well as Co and Mo.

Methods

Using the Materials Project database[22] and following the procedure outlined in Fig. 1, we first selected Co- and Mo-based binary alloys that are both experimentally validated and metallic. Then, alloys containing fewer than 40 sites were selected as candidate materials. It is worth noting that a large number of atoms significantly increases computational cost by complicating charge density calculations and lowering the crystal symmetry. Furthermore, rare-earth and radioactive elements, including those from the lanthanide series, were excluded from candidate materials.

The cohesive energy of binary alloys composed of atoms A and B is calculated as:

$$E^{AB}_{cohesive} = \frac{E^{AB}_{bulk} - \left[xE^{A}_{atom} + yE^{B}_{atom}\right]}{x + y} \quad (3)$$

where E^{AB}_{bulk} is the total energy of the binary alloy, E_{atom} is the energy of the isolated elements A or B, and x and y represent the number of atoms of elements A and B, respectively, in the binary alloy. As described in Fig. 1, the screening criterion was set to cohesive energy greater than 5.5 eV per atom to identify candidates with potential resistance to electromigration. If at least one phase of a binary alloy satisfies this criterion, all associated phases were selected for subsequent calculations.

Regarding $\rho_0\lambda$ in eqn (2), it is intrinsically anisotropic since $v_{n,t}$ depends on the transport direction t. However, considering the random orientation of grains in interconnect metals, we calculated the directionally averaged $v_{n,t}$ by integrating over all

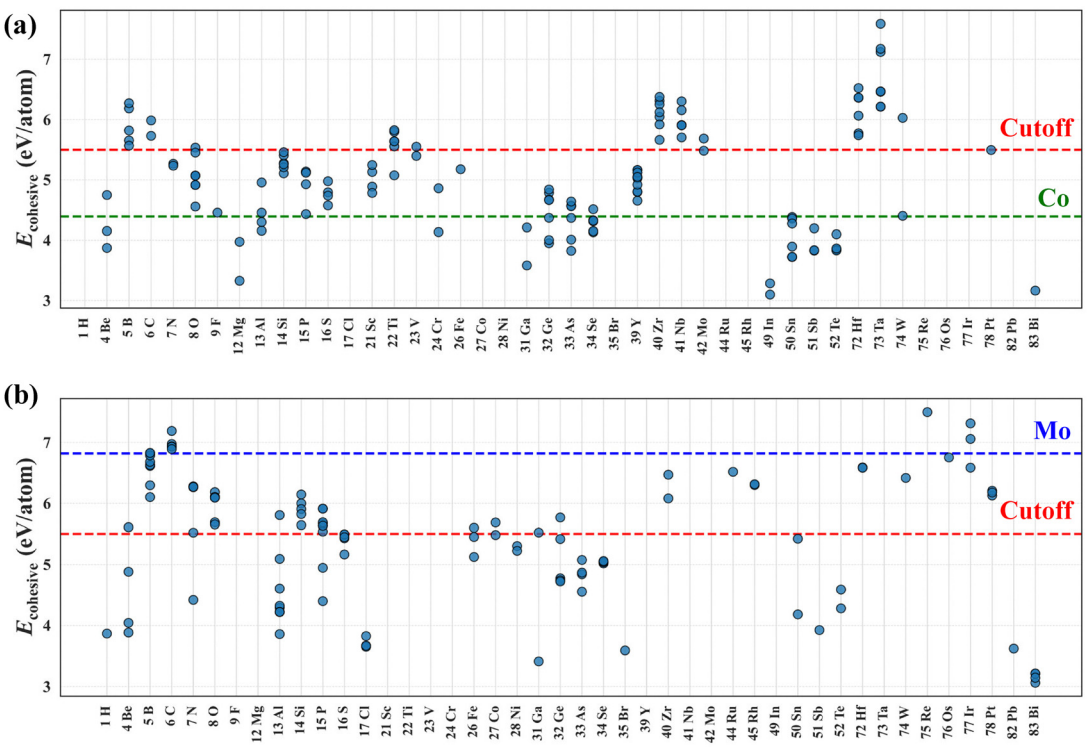

Fig. 2 Cohesive energies of (a) Co-based and (b) Mo-based binary alloys, respectively. The red line indicates a cutoff energy of 5.5 eV per atom. The green and blue lines indicate the cohesive energies of elemental Co (α-phase) and Mo, respectively.

directions on a unit sphere Ω. Specifically, for a given k-point, the directional average of $v_{n,t}$ is given by:

$$\begin{aligned} v_{n,t}{}^2(\boldsymbol{k})_{\text{avg}} &= \frac{1}{4\pi}\iint \mathrm{d}\Omega (v\cdot\boldsymbol{u})^2 \\ &= \frac{1}{4\pi}\int_0^{2\pi}\int_0^{\pi} \sin\theta \mathrm{d}\theta \mathrm{d}\phi \\ &\quad \times \left(v_x \sin\theta\cos\phi + v_y \sin\theta\sin\phi + v_z\cos\theta\right)^2 \\ &= \frac{1}{3}|v_n(\boldsymbol{k})|^2 \end{aligned} \tag{4}$$

where $\boldsymbol{u}$ is the unit vector. Substituting this into eqn (2), the average $(\rho_0\lambda)_{\text{avg}}$ becomes

$$\frac{1}{(\rho_0\lambda)_{\text{avg}}} = \frac{e^2}{4\pi^2\hbar}\cdot\frac{1}{3}A_{\text{f}} \tag{5}$$

where A_{f} is the area of the Fermi surface (FS).

To obtain $(\rho_0\lambda)_{\text{avg}}$, band structures were calculated from DFT calculations using Quantum Espresso.[23] The SSSP precision pseudo potentials[24] were employed for both self-consistent and non-self-consistent calculations. A k-point grid of 40 × 40 × 40 (40^3) was used. Spin-polarized calculations were performed for alloys with magnetic moments greater than $0.05\mu_{\text{B}}$.

Results and discussion

The cohesive energies of Co and Mo binary alloys are shown in Fig. 2(a) and (b), respectively, with a cutoff energy of 5.5 eV per atom. The cutoff value for the cohesive energy was set to 5.5 eV per atom, which lies between that of Cu (3.4 eV per atom) and those of Ru and Mo (6.7 eV per atom), representing a balance between electromigration reliability and process compatibility in ultrathin interconnects. While Cu suffers from severe electromigration issues, excessively high cohesive energies such as those of Ru and Mo may degrade interfacial stability and electrical performance due to film non-uniformity and enhanced grain-boundary scattering.[25,26] The green and blue lines represent the cohesive energies of elemental hexagonal close-packed Co (α-phase) and Mo, which are 4.39 and 6.82 eV per atom, respectively.[27] The distributions shown in Fig. 2 reveal that the following binary alloys are promising candidates, exhibiting cohesive energies greater than 5.5 eV per atom: (a) for Co-based systems, alloys with B, C, O, Ti, V, Zr, Nb, Mo, Hf, Ta, W, and Pt (total 58 alloys); and (b) for Mo-based systems, alloys with Be, B, C, N, O, Al, Si, P, S, Fe, Co, Ga, Ge, Zr, Ru, Rh, Hf, W, Re, Os, Ir, and Pt (total 89 alloys). By excluding alloys composed of 40 or more atoms, the number of candidates is reduced to 57 for Co-based and 78 for Mo-based alloys, respectively.

The averaged FoM, $(\rho_0\lambda)_{\text{avg}}$, are presented alongside the cohesive energies in Fig. 3. The red line indicates FoM of Cu (6.70×10^{-16} Ω m^2). The green and blue lines present FoM of Co (6.13×10^{-16} Ω m^2) and Mo (5.89×10^{-16} Ω m^2), respectively. Cohesive energy and FoM values in Fig. 3 are listed in Tables S1 and S2 in the SI.

In Fig. 3(a), four Co-based binary alloys—CoTi (mp-823), Co_3Ti (mp-608), $CoPt_3$ (mp-922) and CoZr (mp-2283) where 'mp' denotes the material ID from the Materials Project database[16] —exhibit smaller $(\rho_0\lambda)_{\text{avg}}$ than Cu and lower or comparable $(\rho_0\lambda)_{\text{avg}}$ than Co. Furthermore, they have larger cohesive energy than Co. For Mo-based binary alloys, shown in Fig. 3(b), seven alloys—MoC (mp-2746), MoB_2 (mp-960), Mo_2B_5 (mp-7229), MoN (mp-1065394), MoRh (mp-12595), MoW_{11} (mp-1103318), and MoIr (mp-11481) —have smaller $(\rho_0\lambda)_{\text{avg}}$ than Cu. Among these, MoC (mp-2746), MoB_2 (mp-960), and MoN (mp-1065394) exhibit even smaller $(\rho_0\lambda)_{\text{avg}}$ than Mo. Thus, the most promising binary alloys among the candidates are CoTi (mp-823) and MoC (mp-2746). In addition, considering multiple phases, the Co–Ti and Mo–B alloy systems appear to be the best candidates on average. If the cohesive energy cutoff is raised to 6.0 eV per atom, Co–Ti and Co–Pt alloys are excluded making Co–Zr alloys more promising. In contrast, Mo-binaries have no change in determination of candidates.

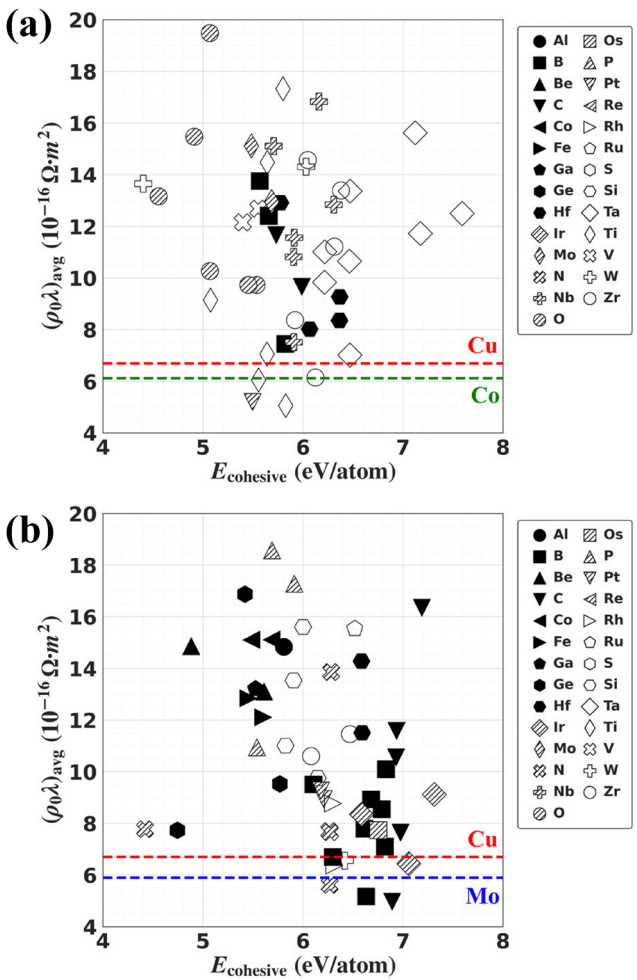

Fig. 3 Averaged FoM and cohesive energies for (a) Co- and (b) Mo-based binary alloy candidates, respectively. Candidates with the averaged FoM value larger than 20 were excluded.

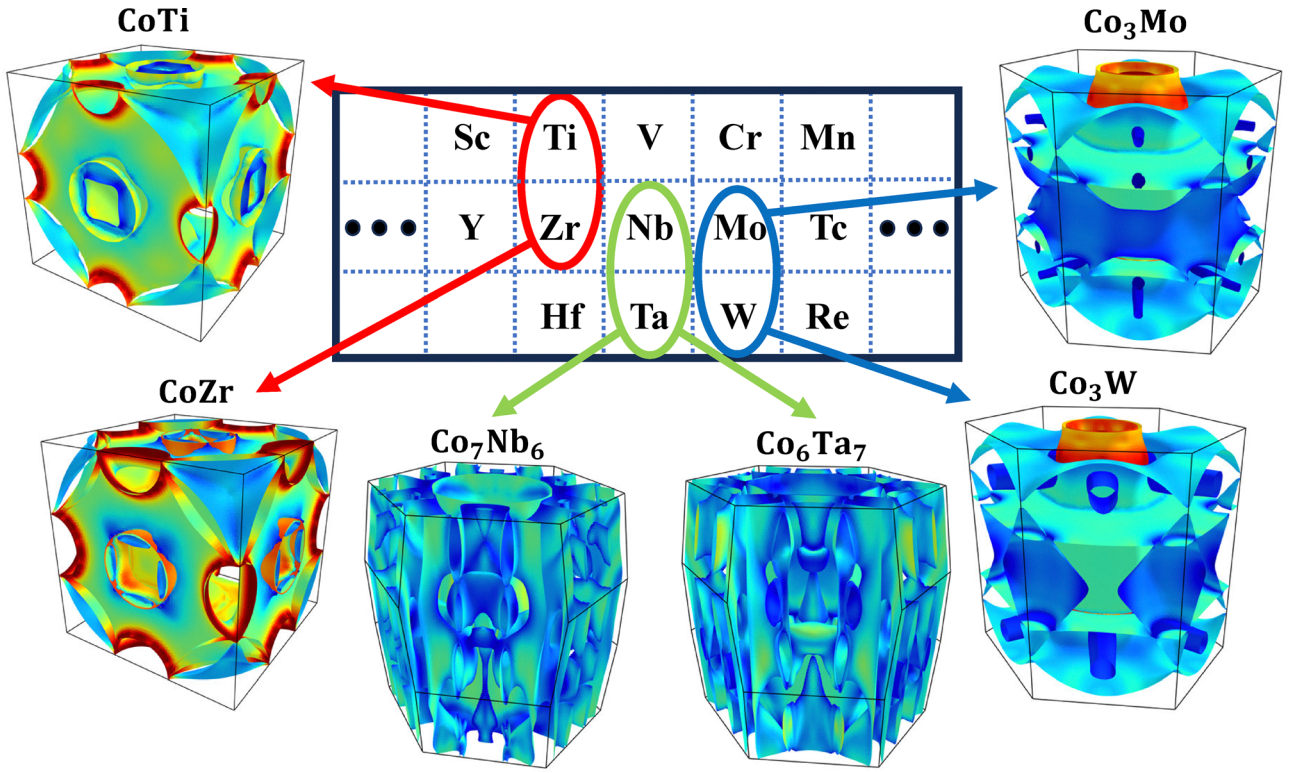

Fig. 4 Fermi surfaces of Co binary alloys. The periodic table includes elements from groups 4, 5, and 6, and periods 4, 5, and 6. The red, green, and blue lines indicate elements belonging to the same group.

Furthermore, the promising Co-based candidates are on the convex hull, indicating thermodynamic stability, except for Co3Ti, which has a small energy-above-hull value of 0.04 eV per atom. In contrast, among the Mo-based candidates, only MoN, MoRh, and MoIr are on the convex hull, while the others exhibit finite energies above the hull: MoC (0.298 eV per atom), MoB2 (0.156 eV per atom), Mo2B5 (0.745 eV per atom), and MoW11 (1.713 eV per atom). Therefore, for these candidates with finite energy-above-hull values, suppressing thermodynamic instability through metastable or kinetic stabilization will be necessary to ensure good device reliability.

In the FoM calculation, similarity in FS leads to similar averaged FoM, $(\rho_0\lambda)_{avg}$, as the metric depends solely on the FS area. Therefore, since the number of outer-shell electrons is the same group in the periodic table tend to exhibit similar FS, as shown in Fig. 4, and consequently similar $(\rho_0\lambda)_{avg}$. Furthermore, if the FS complexity or shape is comparable, a smaller lattice parameter improves FoM because the FS area is inversely proportional to the lattice parameter. Since alloys containing atoms from larger periods generally have larger lattice parameters, it is reasonable to prioritize candidates composed of atoms from the smallest possible periods. The best-performing combinations, CoTi (mp-823) and MoC (mp-2746), are consistent with this reasoning. Nonetheless, better candidates may exist in atomic structures that cannot be formed with such small-period elements.

As described in the Methods section, a 40^3 k-point grid was used in our FoM calculations, whereas a finer than 200^3 grid was employed for elemental metals to achieve convergence of FoM as the surface areas at band crossings are highly sensitive.[6] As shown in Fig. 5, we also performed FoM calculations for selected alloys using a denser k-point grid of up to 200^3, which confirmed that the error remains below 5%, even for the complex FS of $CoPt_3$. Considering the constant mean free path approximation, the calculated value is sufficiently accurate for selecting potential candidates. This is because eqn (2) involves drift velocities that may require finer k-point grids, whereas eqn (5) depends solely on the FS area.

In this work, since the screening was performed using the averaged FoM and cohesive energy, further validation is required, including assessments of interface binding energy with low-k dielectrics, *via* resistance, and grain boundary resistance. Therefore, our calculations should be considered as an initial screening step.

Conclusions

We performed a first-principles screening of Co- and Mo-based binary alloys as advanced interconnect metals. Screening employs FoM, an indicator of the size effect, and cohesive energy, a proxy for electromigration resistance. Several Co- and Mo-based alloys outperform Cu in both FOM and cohesive energy. This result reflects FS similarities, where elements sharing the same group number and crystal structure exhibit comparable FS characteristics, implying that alloys with smaller lattice parameters tend to have better FoM.

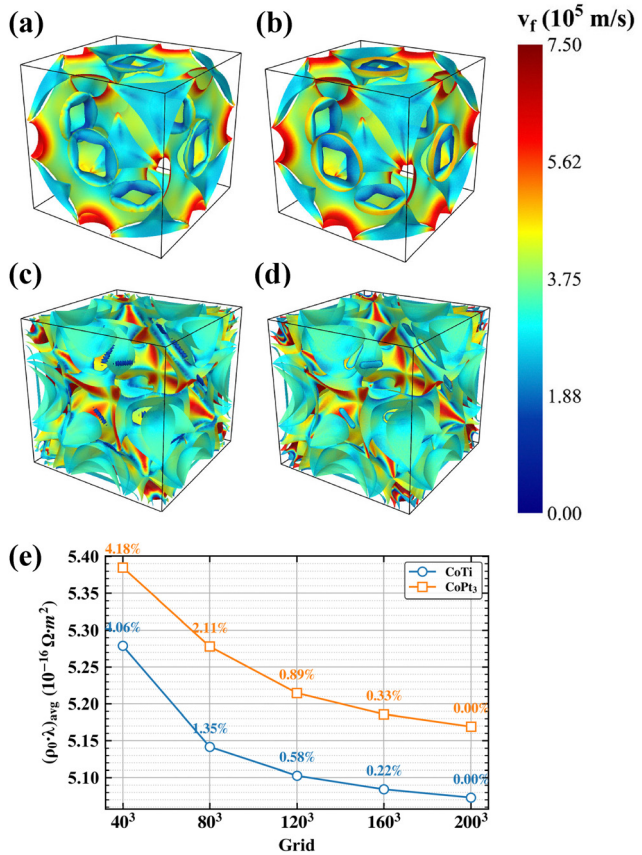

Fig. 5 Fermi surfaces of CoTi calculated with k-point grids of (a) 40^3 and (b) 200^3, and $CoPt_3$ calculated with k-point grids of (c) 40^3 and (d) 200^3. Colors indicate Fermi velocities ranging from 0 to 10^5 m s^{-1}. (e) Relative error of the averaged FoM calculated using different grid densities compared to the 200^3 k-point grid.

Conflicts of interest

There are no conflicts to declare.

Data availability

The data supporting this article have been included as part of the supplementary information (SI). Supplementary information is available. See DOI: https://doi.org/10.1039/d5tc04036a.

Acknowledgements

This research was supported by the Nano & Material Technology Development Program through the National Research Foundation of Korea (NRF) funded by the Ministry of Science and ICT (RS-2024-00407291). This work was also supported by the Technology Innovation Program (“RS-2023-00234828”) funded by the Ministry of Trade, Industry & Energy (MOTIE, Korea) (1415187391).

References

1 K. Fuchs *The conductivity of thin metallic films according to the electron theory of metals*. Mathematical Proceedings of the Cambridge Philosophical Society, Cambridge University Press, 1938, vol. 34, pp 100–108.
2 E. H. Sondheimer, The mean free path of electrons in metals, *Adv. Phys.*, 2001, **50**(6), 499–537.
3 A. Mayadas, M. Shatzkes and J. Janak, Electrical resistivity model for polycrystalline films: the case of specular reflection at external surfaces, *Appl. Phys. Lett.*, 1969, **14**(11), 345–347.
4 A. Mayadas and M. Shatzkes, Electrical-resistivity model for polycrystalline films: the case of arbitrary reflection at external surfaces, *Phys. Rev. B: Solid State*, 1970, **1**(4), 1382.
5 D. Gall, The search for the most conductive metal for narrow interconnect lines, *J. Appl. Phys.*, 2020, **127**(5), 050901.
6 D. Gall, Electron mean free path in elemental metals, *J. Appl. Phys.*, 2016, **119**(8), 085101.
7 S. Kumar, C. Multunas, B. Defay, D. Gall and R. Sundararaman, Ultralow electron-surface scattering in nanoscale metals leveraging Fermi-surface anisotropy, *Phys. Rev. Mater.*, 2022, **6**(8), 085002.
8 K. Sankaran, K. Moors, Z. Tőkei, C. Adelmann and G. Pourtois, Ab initio screening of metallic MAX ceramics for advanced interconnect applications, *Phys. Rev. Mater.*, 2021, **5**(5), 056002.
9 Y. Hu, P. Conlin, Y. Lee, D. Kim and K. Cho, van der Waals 2D metallic materials for low-resistivity interconnects, *J. Mater. Chem. C*, 2022, **10**(14), 5627–5635.
10 G. Cui, Z. Guo, X. Ren, Y. Jiang, X. Jin, Y. Wu and S. Ju, Active Learning for the Discovery of Binary Intermetallic Compounds as Advanced Interconnects, *J. Phys. Chem. Lett.*, 2025, **16**(14), 3579–3588.
11 K. Sankaran, S. Clima, M. Mees and G. Pourtois, Exploring alternative metals to Cu and W for interconnects applications using automated first-principles simulations, *ECS J. Solid State Sci. Technol.*, 2014, **4**(1), N3127.
12 J. R. Lloyd, M. W. Lane, E. G. Liniger, C.-K. Hu, T. M. Shaw and R. Rosenberg, Electromigration and adhesion, *IEEE Trans. Device Mater. Reliab.*, 2005, **5**(1), 113–118.
13 N. Bekiaris, Z. Wu, H. Ren, M. Naik, J. H. Park, M. Lee, T. H. Ha, W. Hou, J. R. Bakke and M. Gage, Cobalt fill for advanced interconnects, in 2017 IEEE international interconnect technology conference (IITC), 2017, IEEE, pp. 1–3.
14 C. Auth, A. Aliyarukunju, M. Asoro, D. Bergstrom, V. Bhagwat, J. Birdsall, N. Bisnik, M. Buehler, V. Chikarmane and G. Ding, A 10 nm high performance and low-power CMOS technology featuring 3rd generation FinFET transistors, Self-Aligned Quad Patterning, contact over active gate and cobalt local interconnects, in 2017 IEEE International Electron Devices Meeting (IEDM), 2017, IEEE, pp. 29.21.21–29.21.24.
15 A. Gupta, J. W. Maes, N. Jourdan, C. Zhu, S. Datta, O. V. Pedreira, Q. T. Le, D. Radisic, N. Heylen and A. Pacco, Barrierless ALD molybdenum for buried power rail and via-to-buried power rail metallization, in 2022 IEEE

International Interconnect Technology Conference (IITC), 2022, IEEE, pp. 58–60.

16 A. Pacco, T. Nakano, A. Iwasaki, S. Iwahata and E. A. Sanchez, Controlled ALE-type recess of molybdenum for future logic and memory applications, in 2021 IEEE International Interconnect Technology Conference (IITC), 2021, IEEE, pp. 1–3.

17 J. H. Moon, E. Jeong, S. Kim, T. Kim, E. Oh, K. Lee, H. Han and Y. K. Kim, Materials quest for advanced interconnect metallization in integrated circuits, *Adv. Sci.*, 2023, **10**(23), 2207321.

18 S. W. Park, H. Han, C. W. Ahn and J. K. Park, Influence of deposition conditions on ALD based Ru passivation for Cu–Cu hybrid bonding, *Sci. Rep.*, 2025, **15**(1), 36620.

19 H. Nakatsubo, D. Mohapatra, E. S. Lee, J. Kim, I. Cho, M. Iseki, T. Shigetomi, R. Harada, S. W. Na and T. Cheon, Small and Simple Molecular Structure Based Thermally Stable Ruthenium Precursor in Advancing Ruthenium ALD Process for Scaled Interconnect Metallization, *Adv. Sci.*, 2025, e19209.

20 E. Cho, W.-J. Son, S. Lee, H.-S. Do, K. Min and D. S. Kim, Unraveling the adhesion characteristics of ruthenium as an advanced metal interconnect material using machine learning potential, *J. Mater. Chem. C*, 2025, **13**(15), 7772–7784.

21 E. Smirnova; A. Miakonkikh, A. Rogozhin and K. Rudenko, Atomic layer deposition of Ruthenium on different interfaces for an advanced metallization system of ICs. In J. Phys.: Conf. Ser., 2020, IOP Publishing: vol. 1695, p. 012045.

22 A. Jain, S. P. Ong, G. Hautier, W. Chen, W. D. Richards, S. Dacek, S. Cholia, D. Gunter, D. Skinner and G. Ceder, Commentary: The Materials Project: A materials genome approach to accelerating materials innovation, *APL Mater.*, 2013, **1**(1), 011002.

23 P. Giannozzi, S. Baroni, N. Bonini, M. Calandra, R. Car, C. Cavazzoni, D. Ceresoli, G. L. Chiarotti, M. Cococcioni and I. Dabo, QUANTUM ESPRESSO: a modular and open-source software project for quantumsimulations of materials, *J. Phys.: Condens. Matter*, 2009, **21**(39), 395502.

24 G. Prandini, A. Marrazzo, I. E. Castelli, N. Mounet and N. Marzari, Precision and efficiency in solid-state pseudopotential calculations, *npj Comput. Mater.*, 2018, **4**(1), 72.

25 X. Li, H. Wu, W. Gao and Q. Jiang, A roadmap from the bond strength to the grain-boundary energies and macro strength of metals, *Nat. Commun.*, 2025, **16**(1), 615.

26 Y. Zhu, X. Lang, W. Zheng and Q. Jiang, Electron scattering and electrical conductance in polycrystalline metallic films and wires: impact of grain boundary scattering related to melting point, *ACS Nano*, 2010, **4**(7), 3781–3788.

27 C. Kittel and P. McEuen, *Introduction to solid state physics*, John Wiley & Sons, 2018.

